Appl Phys B (2012) 108:81–87
DOI 10.1007/s00340-012-5042-5

Applied Physics B
Lasers and Optics

Passive coherent combining of lasers with phase-contrast filtering for enhanced efficiency

F. Jeux · A. Desfarges-Berthelemot · V. Kermène · J. Guillot · A. Barthelemy

Received: 23 January 2012 / Revised version: 2 April 2012 / Published online: 29 May 2012
© Springer-Verlag 2012

Abstract A new passive technique to phase-lock a laser array is proposed and analyzed. It improves the laser combining efficiency with a large number of emitters. Our architecture combines selective coupling based on a phase-contrast filter and resonant phase nonlinearity of amplifiers. A numerical study predicts that with 20 fiber lasers the architecture leads to a phase-locking efficiency which is twice the value observed up to now in published experiments.

1 Introduction

Coherent combining is a means to achieve very high power levels and a high brightness beam from a set of lasers of lower power. The last decade has shown an increasing interest in laser combining, especially with the progress in fiber laser performances and technology. One possible scheme is based on a master oscillator power amplifier (MOPA) arrangement with a set of parallel amplifying arms. The required phase control is performed by an optoelectronic feedback loop including phase-sensitive detection and phase modulators in each amplifier channel. A maximum of 4 kW and 105 kW CW has been demonstrated with fiber laser arrays and bulk laser arrays, respectively, using this kind of technique [1, 2]. The scalability of the active phase control was also demonstrated by the co-phasing of about 50 beams from separate fibers [3] or from separate cores of a single fiber [4]. An attractive and simpler method for laser combining is based on a single and specific cavity design including multiple amplifying branches. Power summation and generation of the phase-locked beam array results from intra-cavity filtering or coupling and selection of the least loss laser pattern. Numerous cavity architectures have been proposed and tested which belong to the class of coherent combining techniques called "passive" or "self-organized" [5–13], e.g., the Talbot cavity, interferometer resonator, Fourier cavity, all-optical feedback loop, and mutual injection, etc. In the field of fiber lasers, 710 W were obtained [11] and an array of 25 lasers [14] was investigated. However, it has been shown that the combining efficiency drops when the array size becomes large (>10). Theoretical papers as well as experiments demonstrated that evolution [14–17]. This trend can be simply explained by the fact that, when increasing the number of subcavities in the laser resonator, it becomes difficult (and at some point even impossible) to find a common frequency which satisfies all the resonance conditions in the amplification bandwidth. The consequence is an increase in laser losses and/or deviation from perfect co-phasing of the output beams. Both lead to a drop in combining efficiency, even though there is still a significant gain in terms of beam brightness with respect to incoherent beam summation. A recent experimental study with up to 16 fiber lasers reported a power combining falling to 55 % compared with 98 % measured with only two lasers in operation. When looking for a combining efficiency greater than 80 %, one should limit the laser architecture to typically 8 to 12 elementary lasers, depending on the various cavity lengths and the spectral bandwidth of concern [17]. It was found that a resonator design with a common feedback to

F. Jeux · A. Desfarges-Berthelemot · V. Kermène · J. Guillot · A. Barthelemy (✉)
XLIM UMR 6172, CNRS—Université de Limoges,
123 Avenue Albert Thomas, 87060 Limoges, France
e-mail: alain.barthelemy@xlim.fr
Fax: +33-555457253

F. Jeux
ASTRIUM SAS, 6 rue L. Pichat, 75016 Paris, France

J. Guillot
CILAS, 8 Avenue Buffon, ZI La Source, 45063 Orléans, France

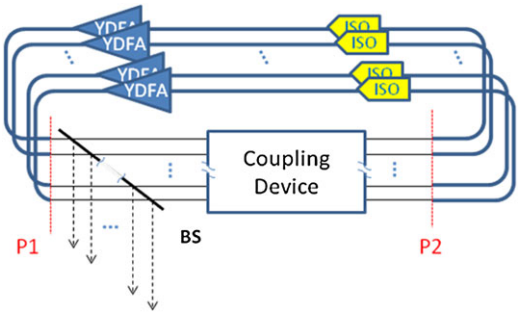

Fig. 1 Schematic of the laser array architecture including fibered (ytterbium-doped fiber amplifiers, isolators) and free space parts

all the amplifying channels ($1 \times N$ geometry) does not offer a sufficient number of degrees of freedom to overcome the limitation of efficiency drop upon number of laser units. In another arrangement, where each laser was coupled to its neighbors, it was shown that increasing the connectivity slightly improved the average phase-locking efficiency [14]. Architectures where each laser arm couples to all others at each round trip ($N \times N$ geometry) could give more degrees of freedom. For instance, in 2008 Corcoran et al. introduced [18] a new version of the self-Fourier cavity design where the free space part and the multiple parallel fiber laser part operate as coupled cavities. The laser array was considered as a set of nonlinear regenerative amplifiers with a random distribution of lengths. A gain-dependent phase shift in a properly engineered configuration compensated for the length differences of the "cold" cavity. Based on a calculation of the stable states of the cavity, their analysis indicated that an in-phase supermode with a high degree of coherence could be obtained even for a large number of elements.

We report in this paper a numerical study on a new cavity design for enhancement of the combining efficiency of a large laser array. It includes multiple optical feedback loops, specific $N \times N$ amplitude and phase coupling between the laser arms and involves resonant nonlinearity of the amplifiers.

2 Proposed laser scheme

Our approach is based on a ring cavity configuration schematically depicted on Fig. 1. Amplification is provided by an array of N parallel fiber amplifiers (YDFA) characterized by nearly similar small signal gain and saturation power but with nonidentical lengths. In practice, it appears unrealistic to cut all the fiber amplifying arms at the same length within a fraction of the wavelength and to keep it identical without a servo control. Unidirectional operation of the ring laser is ensured by optical isolators (ISO) inserted in each of the fiber amplifiers. The major part of the amplifier output power is coupled out of the cavity by a beam splitter (BS). The small fraction of power which is transmitted by the beam splitter goes through a device introducing coupling between the different arms before feeding the fiber array for laser oscillation. In the absence of coupling, each amplifier arm oscillates independently, and the system delivers an incoherent array of N laser beams. Laser fields can be coupled, for instance, through diffraction and/or spatial filtering in the far field. As one example of the latter case, the plane wave spectrum of the laser beam array can be displayed in the common focal plane of telescope lenses. A simple pinhole transmitting only the central part of the far field can achieve the phase coupling required to get emission of an in-phase supermode. For a proper dimension of the filter (hole diameter of the order of the width of the main lobe of the fundamental supermode diffraction pattern) the laser field launched into the different amplifiers carries the same frequency and phase information. Because it relies on the same basic principle, this arrangement will operate exactly like the configuration previously reported in [10] and [11], where the spatial filtering was performed by a single-mode fiber. To go beyond this scheme of common feedback ($1 \times N$ coupling) we propose the following approach. First we assume that the different laser beams will produce approximately similar powers because the fiber amplifiers are of comparable performance. Then, we transform the phase difference between the individual beams at the fiber outputs (P1 plan) into amplitude deviation at the input of the amplifiers (P2 plan), due to the coupling device. Consequently, the gain provided by each amplifier until saturation will slightly vary from one to another. Resonant nonlinearity in the amplifiers, i.e., the contribution of the population inversion to the refractive index, gives in the present case a crucial gain-dependent phase shift. The nonlinear phase shifts in turn reduce the linear phase deviations among the laser output beam array due to path length differences. The process is iterated and leads to a stable co-phased beam pattern for proper setting of the laser parameters. There are several possible ways to implement the phase-to-amplitude conversion. The spatial filtering we suggest was inspired by the principle of phase-contrast microscopy due to F. Zernike [19]. It translates faint phase changes into intensity modulations. The technique has been used for a long time for imaging the phase structure of thin and transparent objects. The microscope includes a phase plate in the focal plane of a relay lens to shift the phase of the direct light (central part of the far field) by $\pi/2$ from the diffracted part. The spatial filter we propose is slightly different. It combines phase filtering of only the central part of the diffraction pattern with attenuation of the side lobes. The associated coupling matrix $[C]$ relating the amplitude of the different outputs of the amplifier array to the array inputs is a square matrix of size N for

a one-dimensional (1D) array of N lasers. It can be written as follows:

$$[C] = \beta \cdot [I] - \frac{\beta - e^{i\pi/2}}{N} \cdot [\mathbf{1}]$$

where β stands for the attenuation of the high spatial frequency, $[I]$ denotes the unit matrix, and $[\mathbf{1}]$ is a square matrix with all the elements equal to one. For comparison, the coupling matrix of a pinhole filter giving a common feedback for all branches of the laser ($1 \times N$ scheme) is simply described by:

$$[C] = (1/N) \cdot [\mathbf{1}]$$

The investigations on the above-described laser scheme were based on numerical modeling which is presented in the following section.

3 Modeling

Our model simulates the operation of a laser with multiple parallel paths. It computes the buildup of the laser field starting from a noise-like input, which mimics spontaneous emission from the amplifiers, until a steady state is reached. Frequency filtering as well as spatial filtering and beam coupling are included. To make the computations closer to reality we have included in the coupling matrix the impact of diffraction from the far field spatial filter. Fiber lengths, gain saturation, and gain-dependent phase shift are also taken into account using the standard relationships:

$$g = g_0 \cdot \left(\frac{1}{1 + I/I_{\text{sat}}} \right) \quad \text{and} \quad \Phi_{\text{gain-dependent}} = \gamma \cdot g \cdot L_{\text{amp}}$$

where g_0 is the small signal gain, I_{sat} is the saturation intensity, both being chosen identical for the whole set of amplifiers, L_{amp} stands for the amplifiers' active length, and γ for the ratio between real and imaginary part of the susceptibility. The parameter γ varies strongly with frequency, especially in the vicinity of the resonance associated with the laser transition [20, 21]. However, high power ytterbium fiber lasers usually operate in the range 1060–1080 nm, i.e., far from the strong resonance at 980 nm. Based on Ref. [22], where the Yb spectral line shape is expanded in a sum of Lorentzian contributions, we set the parameter γ close to one as a typical value. Therefore, the electronic contribution of Yb ions to the optical phase is reduced when the gain saturates. Outcoupling and additional roundtrip intra-cavity losses are included through a field attenuation coefficient α.

For each frequency, chosen one by one in a selected frequency range, we repeated our computational procedure. We started from a noise of constant intensity but random phase with a uniform distribution. Assuming that gain competition will favor the state giving the highest output power with the fastest buildup dynamics, we identified the corresponding state(s) and their associated frequencies as the actual laser mode(s) expected in practice.

4 Results and discussion

As a preliminary test, the model was used to study the behavior of a cavity with a common feedback to all the parallel branches, since that configuration has been already investigated by several authors. It is worth mentioning that the limitation encountered with this design is also shared by other classes of laser cavities [9, 14, 17] because they are ruled out by the same basic physics [15]. Thus the results served as a reference for comparison with the behavior of a laser based on the new scheme. In a first set of numerical simulations we studied the laser frequency filtering. Parameters were chosen to fit in the computation window and were as follows: fiber lengths randomly chosen between 10 and 12 meters, wavelength bandwidth of 0.4 nm around 1060 nm central wavelength, integrated small signal gain of 19 dB, $\alpha = 0.02$, resonant nonlinearity $\gamma = 1$. The simulation outcomes varied due to the random choice of fiber lengths. In a first step we selected a set of arm lengths giving typical results and kept it fixed for a valuable comparison between the different laser cavity performances.

A typical result for a 20 fiber amplifier laser is shown on Fig. 2 for both a standard pinhole filtering ($1 \times N$) configuration and the new phase-contrast scheme. The figure displays the starting dynamics of the laser emission for each wavelength, with the evolution of the output laser power on approximately 50 cavity roundtrips until a steady state is reached. Only a fraction (25 pm) of the explored frequency range is given on the figure for clarity. The left part of the figure corresponds to a standard configuration with common feedback (pinhole filtering, $1 \times N$). It should be noted that with the chosen set of fiber lengths it is almost impossible to find an actual common resonance frequency among the longitudinal modes of the 20 individual laser arms. The best frequency matching leads, however, to laser oscillation, selecting a few frequencies for which a steady-state power and beam pattern is achieved. It appears that with the chosen set of parameters a single frequency line was selected here in the frequency range shown on Fig. 2. Keeping the same choice of fiber lengths and gain, the computation made with the new scheme indicated that more lines are oscillating (see right part of Fig. 2). However, the frequency carrying the strongest power, first reaching steady state, is still the same and is likely to be filtered out in practice because of gain competition. A larger difference appears when we calculate the combining efficiency for the frequencies under consideration. The combining efficiency is defined by the on-axis peak power in the plane wave spectrum after normalization. The aperture filling and the overall power are taken into account in the normalization so that, for a perfectly phased array, the combining efficiency should be equal to one. The plots are reported on Fig. 3 and correspond to simulations made with the same parameters and computation window as

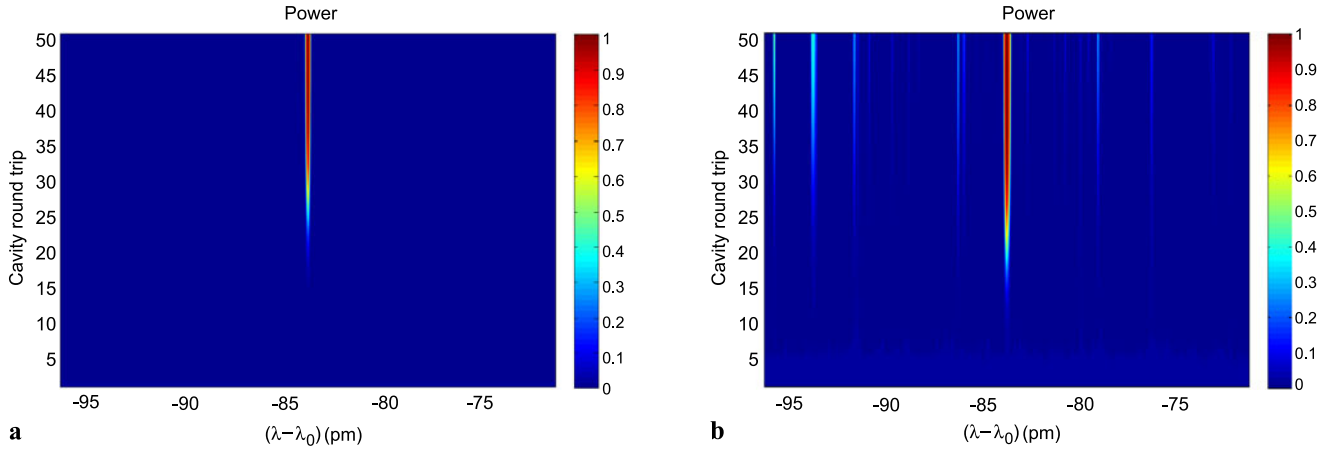

Fig. 2 Evolution of the power of a 20 laser array in a 25 pm wavelength range (*horizontal axis*) according to cavity roundtrip (*vertical axis*) with pinhole coupling on the *left* and with $N \times N$ phase-contrast coupling ($\beta = 0.7$) on the *right*

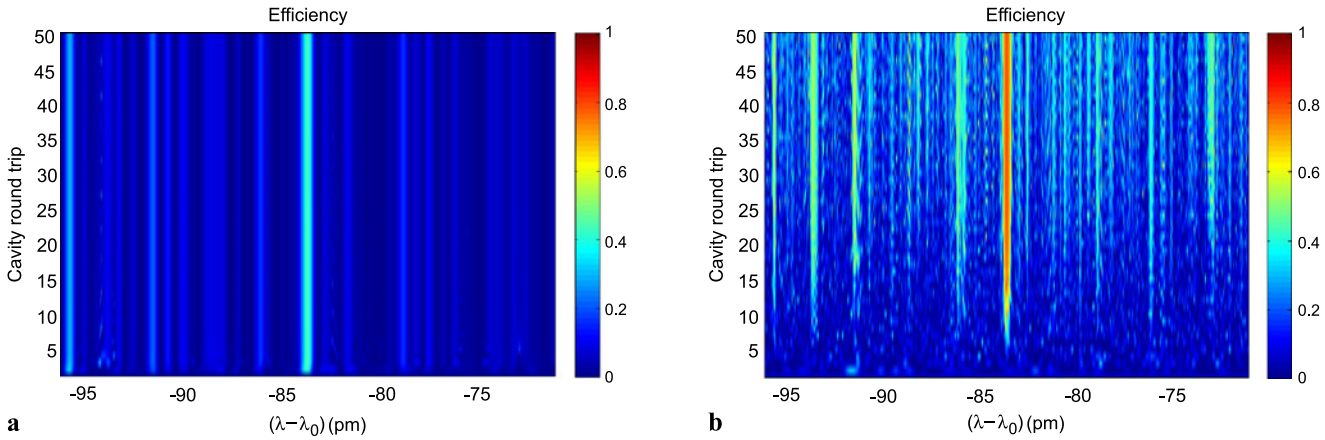

Fig. 3 Evolution of the 20 laser combining efficiency in a 25 pm wavelength range (*horizontal axis*) according to cavity roundtrip (*vertical axis*) with common feedback (pinhole filter) on the *left* and with $N \times N$ coupling (phase-contrast filter with $\beta = 0.7$) on the *right*

for Fig. 2. With the two architectures a single preferred frequency gives the highest efficiency. It is directly related to the frequency reaching oscillation with the fastest rise time in terms of power. However, the peak efficiency is nearly two times larger for the new configuration (nearly 80 % compared to 45 % for the common feedback version). In addition, the dynamics of the laser fields' buildup are also different, as shown on Fig. 4. Again, the two parts of the figure are connected with the two laser arrangements and correspond to the selected wavelength giving rise to the highest power. The continuous line gives the evolution of the normalized power according to the cavity roundtrips, and the dashed line plots the evolution of the combining efficiency. For the standard common feedback scheme (pinhole filtering), computations indicate that phase-locking between the individual outputs (to the best extent permitted by the overlap of longitudinal modes) occurs very fast and well in advance of the power saturation. A similar conclusion was obtained from a different numerical model [17]. For the new phase-contrast filtering cavity, after some preliminary transients, the combining efficiency evolves smoothly toward a steady state. The final value is reached during the last roundtrips before saturation of the emitted power.

The power pattern of the 20 lasers array is shown on Fig. 5, compared for the two schemes at steady state. The common feedback configuration leads to a nearly uniform sharing of the laser power between the different outputs (see Fig. 5, upper panel). In striking difference to the previous case, the phase-contrast architecture gives a nonuniform intensity across the array (see Fig. 5, lower panel). This was expected, because this is the extra degree of freedom provided by the new configuration. Variations in power compensate for the differences in optical path in the fiber array, through power-dependent phase shift in the amplifiers. Despite the nonuniformity of the power profile, the total extracted power with the phase-contrast filtering is improved in comparison with the pinhole coupling because of lower filtering losses. In addition, the improvement in phase uni-

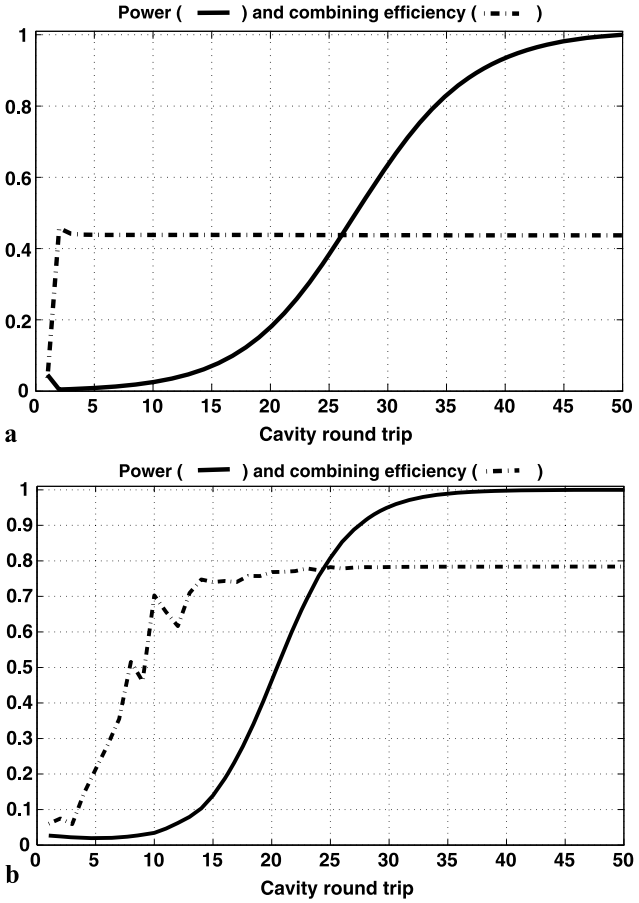

Fig. 4 Power (*continuous line*) and combining efficiency (*dashed line*) of the 20 laser array according to cavity roundtrip with common feedback (pinhole filter) on the *top* and with $N \times N$ coupling (phase-contrast filter) on the *bottom*

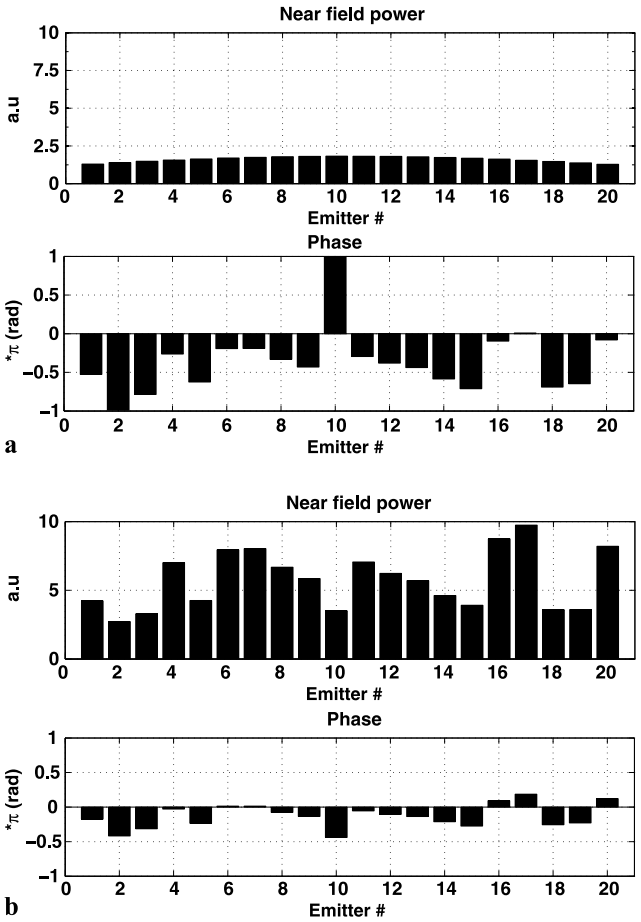

Fig. 5 Near field power and phase profiles at steady state for an array of 20 lasers with a cavity including a common feedback by means of pinhole filtering (*upper panel*) and for a phase-contrast filtering architecture (*lower panel*) for an identical set of parameters

formity and hence in combining efficiency (almost doubled) gives a sixfold enhancement in laser beam brightness with the chosen set of parameters. The far field intensity corresponding to the steady-state pattern of Fig. 5, lower panel, is plotted on Fig. 6, where a periodic distribution of Gaussian elementary beams together with a filling factor of 2.2 have been considered. The profile confirms that the inhomogeneous power distribution in the near field has a very weak impact on the far field, which is a well-known phenomenon, and that the remaining phase deviations are sufficiently low to keep a narrow peak in the plane wave spectrum.

Calculations were then carried out for various numbers of amplifiers N. We fixed the wavelength range to 1060–1065 nm, and the β parameter of the phase-contrast filter was set to 0.5. For each N value we run the simulation 20 times with a different random sampling of the fiber length difference (within the same domain 0–2 m) to have a reliable statistics and to account for the unavoidable path length fluctuations due to environmental perturbations. We then derived the evolution of the average value of the combining efficiency according to the number of laser arms. The

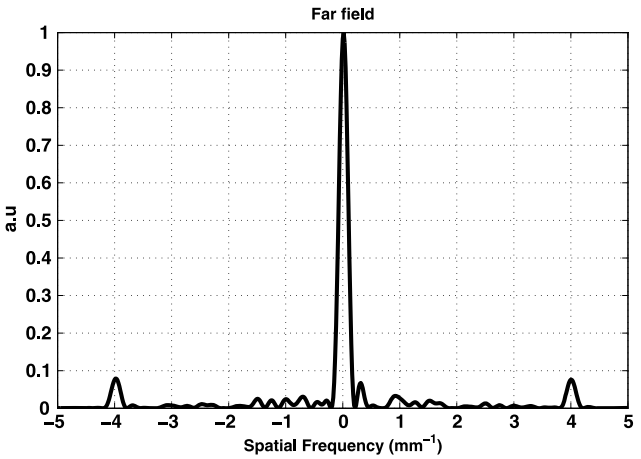

Fig. 6 Normalized far field pattern corresponding to the near field power and phase distributions shown in Fig. 5 lower panel. Gaussian laser beams and a filling factor of (1/2.2) have been assumed

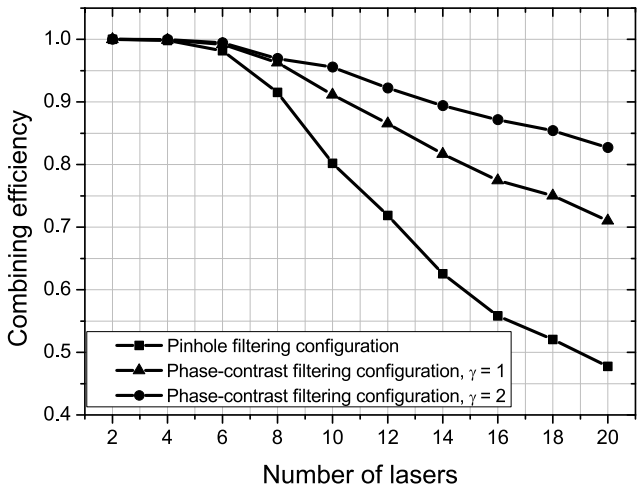

Fig. 7 Combining efficiency according to N, the number of lasers, in the array calculated for pinhole filtering (common feedback) and phase-contrast filtering ($N \times N$) schemes for two values of the nonlinear coefficient γ

curve shown in Fig. 7 with square dots corresponds to a laser configuration with a common feedback for all elements. It shows a decrease in the combining efficiency below 50 % with respect to an increasing number of lasers up to 20. This drop was expected and is consistent with previously published works as well as with experimental observations (see for instance [14] and [17]). We can therefore trust in our modeling. Another series of numerical simulations, related to the phase-contrast coupling scheme, served to get a picture of the improvement. In comparison with the pinhole filter configuration, a significant enhancement of the efficiency was obtained which started with arrays of 8 to 10 lasers and then increased with the array size. Furthermore, the gain in efficiency evolves with the nonlinearity level. As shown by the two curves of Fig. 7 corresponding to gain-dependent nonlinearity of 1 (triangle dots) and 2 (round dots), the higher the nonlinearity the better the efficiency. For 20 amplified arms, despite the limited frequency window (5 nm) the combining efficiency is improved by more than 80 % with the proposed scheme taking into account a nonlinear coefficient $\gamma = 2$. We have not extended our study beyond $N = 20$ lasers because it is time consuming and also because, with the resonant nonlinearity expected from ytterbium amplifiers, the proposed scheme is not able to recover a perfect phase-locking (100 % combining efficiency). That point deserves deeper investigation, in particular to derive the conditions leading to a stronger nonlinearity. We plan to carry out a series of experiments to characterize the gain-dependent phase contributions of the fiber amplifiers to see if they agree with the current theoretical model.

In any case, the graph of Fig. 7 clearly shows the advantage of the phase-contrast laser scheme to better phase-lock the emission of multiple lasers without any servo control.

5 Conclusion

We have proposed a new cavity design for passive phase-locking of laser arrays in terms of coherent combining of their power in the far field. The new scheme involves a coupling device, performing a phase-to-amplitude transform, and a gain-dependent phase shift introduced by the amplifiers. The cavity design and nonlinearity provide a kind of phase-pulling effect in the spatial domain which compensates for linear phase deviations across the array. It can be somehow compared to the frequency-pulling effect observed in a single-mode laser in the frequency domain. Our numerical simulations show that the proposed cavity improves the phase-locking of a laser array for a large number of lasers in comparison with most of the architectures researched up to now. An improvement of more than 80 % in terms of combining efficiency has been predicted for $N = 20$ lasers. We expect further improvements with an optimized configuration. The benefit of the investigated principle increases for stronger nonlinearity from the gain media. The magnitude of actual resonant nonlinearity that could be found in practice should be clarified in the future. Other types of nonlinear phase contributions could also be exploited with the same goal of balancing the linear phase difference among lasers. Our numerical study has been limited up to now to a 1D array to simplify computations, but it is straightforward to extend the approach to a 2D array. The proposed scheme can be experimentally implemented in various ways, such as far field filtering and diffractive components. Experiments are planned in the near future to confirm the expectations derived from our theoretical study. Our results as well as the ones obtained with a phase conjugate resonator [23] and a self-Fourier cavity [18] seem to confirm that nonlinearity engineered in a proper way offers the only means for eliminating the standard limitations encountered for passive phase-locking of laser arrays of large size.

Acknowledgements The authors thank ASTRIUM and CILAS for their support in the present study.

References

1. C.X. Yu, S.J. Augst, S.M. Redmond, K.C. Goldizen, D.V. Murphy, A. Sanchez, T.Y. Fan, Opt. Lett. **36**, 2686 (2011)
2. M. Wickham, in *Conference on Lasers and Electro-Optics, Paper CThG2*, San Jose (2010)
3. C.X. Yu, J.E. Kansky, S.E.J. Shaw, D.V. Murphy, C. Higgs, Electron. Lett. **42**, 1024 (2006)
4. J. Lhermite, E. Suran, V. Kermene, F. Louradour, A. Desfarges-Berthelemot, A. Barthélémy, Opt. Express **18**, 4783 (2010)
5. L. Michaille, C.R. Bennett, D.M. Taylor, T.J. Shepherd, J. Broeng, H.R. Simonsen, A. Petersson, Opt. Lett. **30**, 1668 (2005)
6. D. Sabourdy, V. Kermene, A. Desfarges-Berthelemot, A. Barthélémy, Electron. Lett. **38**, 692 (2002)
7. A. Shirakawa, T. Saitou, T. Sekiguchi, K. Ueda, Opt. Express **10**, 1167 (2002)

8. B. Colombeau, M. Vampouille, V. Kermene, A. Desfarges, C. Froehly, Pure Appl. Opt. **3**, 757 (1994)
9. C.J. Corcoran, F. Durville, Appl. Opt. **86**, 201118 (2005)
10. J. Lhermite, A. Desfarges-Berthelemot, V. Kermène, A. Barthélémy, Opt. Lett. **32**, 1842 (2007)
11. T.H. Loftus, A.M. Thomas, M. Nosen, J.D. Minelly, P. Jones, E. Honea, S.A. Shakir, S. Hendow, W. Culver, B. Nelson, M. Fitelson, in *Advanced Solid-States Photonics, Paper WA4*, Nara (2008)
12. S. Auroux, V. Kermène, A. Desfarges-Berthelemot, A. Barthelemy, Opt. Express **17**, 17694 (2009)
13. E. Ronen, A.A. Ishaaya, Opt. Express **19**, 1510 (2011)
14. M. Fridman, M. Nixon, N. Davidson, A.A. Friesem, Opt. Lett. **35**, 1434 (2010)
15. D. Kouznetsov, J. Bisson, A. Shirakawa, K. Ueda, Opt. Rev. **12**, 445 (2005)
16. J.E. Rothenberg, Proc. SPIE **6873**, 687315 (2008)
17. W.-z. Chang, T.-w. Wu, H.G. Winful, A. Galvanauskas, Opt. Express **18**, 9634 (2010)
18. C.J. Corcoran, F. Durville, K.A. Pasch, IEEE J. Quantum Electron. **44**, 275 (2008)
19. F. Zernike, Physica **9**, 686 (1942)
20. J.W. Arkwright, P. Elango, G.R. Atkins, T. Whitbread, M.J.F. Digonnet, J. Lightwave Technol. **16**, 798 (1998)
21. A.A. Fotiadi, O.L. Antipov, P. Mégret, Opt. Express **16**, 12658 (2008)
22. C.J. Corcoran, F. Durville, IEEE J. Sel. Top. Quantum Electron. **15**, 294 (2009)
23. P.C. Shardlow, M.J. Damzen, Opt. Lett. **35**, 1082 (2011)